17

Properties and Numerical Modeling-Simulation of Phase Changes Material

Pavel Fiala, Ivo Behunek and Petr Drexler
Brno univerzity of technology, Faculty of electrical engineering and communication, Department of theoretical and experimental electrical engineering, Kolejni 4, Brno Czech Republic

1. Introduction

There exists a domain of models that is principially classified into the linear and non-linear fields of modelling. In the field of non-linear modelling, significant progress has been made since the 1960s thanks to the widespread and regularly available computer technology. This dynamic development influenced a large number of problems including the description of physical behaviour of non-trivial tasks. Non-linear models are solved in the material, spatial, and time domains. However, certain non-linear model domains are not sufficiently developed or regularly used for analysis of the more simple tasks. This group includes task models using non-linear discontinuous characteristics of materials, which can be exemplified by the change of state of a material during heating or cooling. In this section, we would like to use several descriptive examples to expose the problem of thermal tasks solution utilizing applied materials with a phase change (PCM) (Gille, T.; at al. 2007, Volle, F. at al. 2010, Shi, L.P.; at al. 2006). These are mostly coupled tasks (Fiala,P. December 1998). Within the specification of different aspects of the solution process, emphasis will be placed on the final accuracy of the results of numerical analyses, and therefore (rather than focusing on a complete description of the model) the text will accentuate problematic spots within the solution of such tasks.
The PCM characteristics are demonstrated on the task of designing a low-temperature accumulator, an efficient cooler of electronic components, and a separator of impurities in an industrial oil emulsion.

1.1 Energy, transformation, accumulation

Within the last decade, scientific interest in the fields of basic and applied research has been focused more intensively on the problem of increasing the share of renewable sources of energy in total energy consumption per capita (Solar energy 2010). In this context, we have seen major development in the field of energy harvesting (Murat Kenisarin, & Khamid Mahkamov May 2006, John Greenman at al. May 2005, Junrui Liang & Wei-Hsin Liao 2010, Vijay Raghunathan at al. April 2005, Jirku T at al. May 2010), or the acquirement of energy from hitherto unused forms. The reason for such processes in technology naturally consists in the fact that the reserves of classical primary sources of energy and fossil fuels (Behunek, I. 2002, WORLD ENERGY STATISTICS from the IEA 2002) available to current industrial

society are limited. Moreover, such classification applies also to the possibilities of utilizing the energy of water and wind.
A large number of countries have committed themselves to the reduction of greenhouse gas emissions and the related increase of renewable sources of energy (Ministery of industry and trade of Czech Republic, Stat energetic conception 2004, Ministery of industry and trade of Czech Republic 2000) share in total energy consumption. However, the effort to comply with these commitments may be realized in absurd ways such as an uncontrolled surge in the number of constructed solar photovoltaic systems, which is further aggravated by the related problem of their integration into the energy production system of a country, Fig. 1.

Fig. 1. A photovoltaic power plant design, the Czech Republic

One of the applicable alternative source solutions consist in utilizing solar radiation (Solar energy, 2010) within its entire spectrum. Among the advantages of this energy harvesting method there are mainly the low cost of the impinging energy, the unimpeded availability of the source in many regions of the Earth, and the polution-free operation. Conversely, the related disadvantages can be identified in the low density of the impinging radiation power flow in the visible and the near-visible spectrum ($\lambda \in <440,780>$ nm), the comparatively low efficiency of transformation into other forms of energy (considering the currently used photovoltaic elements), and the fact that the cost of a produced energy unit is often rather high when compared to other clean sources of electrical energy (such as nuclear power plants) (Kleczek, J. 1981). In consequence of the uneven power flow density of the solar source within the daily or yearly cycle and owing to weather changes, the solar energy application method is affected by the problems of effective utilization, regulation in power systems, and necessity of accumulating the energy acquired from solar radiation.
A feasible technique of energy accumulation seems to consist in direct exploitation of physical effect of material properties as related to metals, liquids and gases (Gille, T. 2007, Shi, L.P. 2006). Accumulators will facilitate power take-off during any time period depending on the needs of the consumer or the power system operator, which provides for the balance in the cost/power take-off relation within the required time interval. Thus, the power distribution network stability will be improved, with substantial reduction of the probability of black-out (Black-out 2003). There occurs the compensation of time disproportion between the potential of the sources and the eletrical energy on the one hand and the consumption in time and place on the other. Solar energy accumulation can be technologically realized through a wide variety of methods; also, research in the field is

being consistently developed (Juodkazis, Saulius; at al. November 2004, Zhen Ren at al. Januar 2010, Liu, Y.-T.; at al. 2008).
Some of the proposed approaches are based on classical solutions. These include the accumulation of energy utilizing the potential energy of mass in a gravitational field (water), the kinetic energy of mass (flywheels), the non-linearities in the state of a mass phase – the compression of gases. Another group of accumulators is based on the solution utilizing the energy of an electromagnetic field. In this case, the most common is the application of electric accumulators or microbiological systems [mikrobiolog akumulator]. Yet another one of the fields to be quoted comprises energy accumulation using the properties of chemical bonds of non-trivial chemical systems (the production of synthetic fuels), electrochemical bonds, and the utilization of photochemical energy (the accumulation of low-potential heat in solar-powered systems).
The process of designing chemical accumulator forms utilizes the physical effects of non-linear behaviour of materials at phase changes. (Behunek,I. April 2004, Behunek I & Fiala P. Jun 2007).

2. Heat accumulation

Principles are known (Baylin, F. 1979) for the utilization of characteristics of chemical-physical effects, and in this context there exist four basic methods of thermal energy accumulation. The first method consists in the utilization of specific thermal capacity of substances (sensible heat), the second one is built on the application of change in the state of substances (latent heat) , the third one lies in the thermochemical reaction, and the fourth one applies the sorption and desorption of gas / water vapour.
Generally, the thermochemical reactions method provides a higher density of accumulated energy than the sensible heat or phase change options (Mar, R.W. & Bramletta, T.T. 1980). An endothermic reaction product contains energy in the form of a chemical bond that is released retroactively during an exothermic reaction. The energy release occurs through the action of a catalyst, which is a suitable characteristic for long-term accumulation. Other advantages of thermochemical accumulation include the possibility of transporting the products over long distances, the possibility of product storage at both low (with a low rate of loss) and very high temperatures (Goldstein, M. 1961), the low cost, and the fact that products of the reaction can be used as the medium in thermodynamic cycles (The Australian National University 2004). Currently, research (Mar, R.W. 1978, Mar, R.W. 1980) is conducted in this field. In order to accumulate energy, we can utilize heat balance at sorption/desorption of moisture in the working substance. The difference with respect to other types of heat accumulation consists in the fact that sorption does not directly depend on the temperature,. but rather on relative humidity of the surrounding air. Therefore, the described method of accumulation may be realized at a constant temperature, which is an aspect utilizable in discharging the accumulator. In the progress of charging, relative humidity of air is decreased to the required level through heating the air to achieve a higher temperature (Close, D.J. & Dunkle, R.V. 1977, Verdonschet, J.K.M. 1981).

2.1 Classical heat accumulation methods

The classical accumulation of heat utilizes the so-called sensible heat of substances (Kleczek, J., 1981) being the simplest one of all the methods, this approach was historically used in the first place. Traditional materials applied for the accumulation of heat are water and gravel.

The weight and specific heat capacity of these materials indicate the accumulable quantity of heat. This quantity is given by the calorimetric equation

$$Q = \int_{T_1}^{T_2} V \rho c \mathrm{d}T \tag{1}$$

where T_1 is the temperature at the beginning and T_2 the temperature at the end of charging.

2.2 Water heat reservoirs

If water is utilized in the process of accumulation, it is usually held in a suitable container during heating (Garg, H.P., at al. 1985). Even though the applicaton of water has proved to be advantageous in many respects, there are also many drawbacks, especially for the preservation of low-potential heat. Water has the highest specific heat capacity of all known substances (Vohlídal J. et al. 1999). It can be applied as an accumulation and working medium (exchangers are not necessary); charging and discharging can be simulated in an exact manner. If water is applied, heat storage or offtake causes temperature fluctuation and the thermal potential is lost (namely the accumulator is charged at a sufficiently high input temperature T, which is averaged in the reservoir to a mean temperature $T_{stř}$ and, during the subsequent heat offtake, the original temperature T can not be reached) (Fisher L.S. 1976, Lavan, Z. & Thomson, J. 1977). With water accumulators, liquid photothermal collectors need to be applied; this means that expensive and rather complicated technologie and installation methods are used as opposed to the hot.-air option) .

2.3 Gravel heat accumulators

For multi-day or seasonal accumulation (Behunek, I. April 2004), heat reservoris utilizing gravel are preferred; here, the air used as the heating medium is heated in hot-air collectors. This system eliminates some of the disadvantages of the previously described method. In regular realizations, Figure 2, heat transfer by conduction is also minimal (the individual gravel pieces touch one another only at the edges); here, however, the characteristics include low heat capacity of the crushed stone (excessive dimensions of the reservoir) as well as a very difficult (even impossible as per (Garg, H.P., et al. 1985) simulation of charging and discharging.

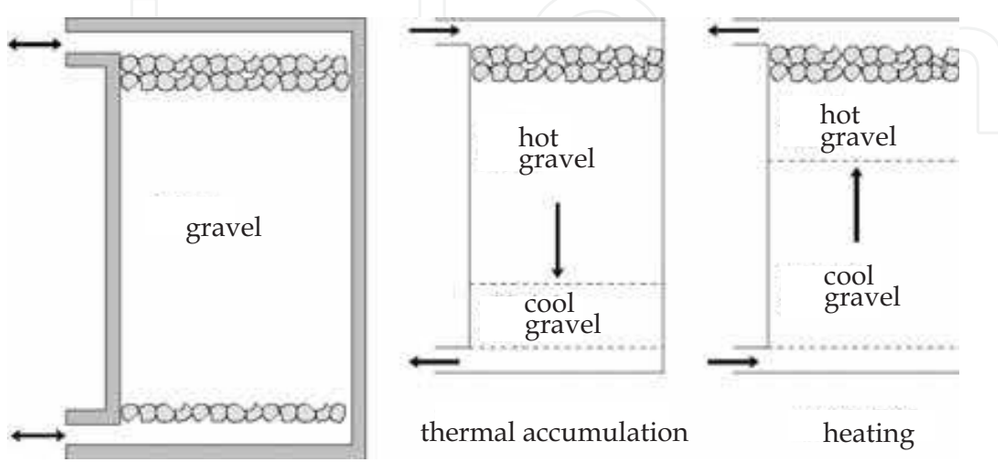

Fig. 2. Schematic description of a heat accumulator using gravel

2.4 Utilizing the change of state in substances for the accumulation of heat

A prospective method of heat accumulation consists in utilizing the change of state of a substance used in a heat reservoir. Such reservoir charges (fillings) are described by the abbreviation PCM (Phase Change Material). According to Ehrenfest (Mechlova, E., Kostal, K. 1999), the changes of state are among the first type of phase changes, where the change of internal energy and substance volume occurs through a jump. If specific melting heat or solidification of the given substance is utilized, the calorimetry equation assumes the form

$$Q = \rho V \Delta h_{\mathrm{m}} + \int_{T_0}^{T_{\mathrm{m}}} V \rho c \mathrm{d}T + \int_{T_{\mathrm{m}}}^{T_{\mathrm{e}}} V \rho c \mathrm{d}T \tag{2}$$

where ρ is the density, V the volume, c the specific heat, Δh_{m} the enthalpy, Q the heat, and T_{m} , T_{e} the temperature according to Figure 3. If heat is supplied to the material, there occurs the transformation from the liquid into the solid state. Phase transition appears when crystal lattice is disrupted, namely when the amplitude of the crystal lattice particles oscillation is comparable with relative distance between the particles. At this moment, the oscillation energy rises above the value of the crystal binding energy, the bond is broken and the crystal transforms into the liquid phase. However, if heat is removed from the substance, there occurs the solidification (crystallization) of material. During crystallization, the orderly motion of molecules gradually assumes the character of thermal oscillations around certain middle positions, namely crystal lattice is formed. In pure crystalline substances, melting and solidification proceed at a constant temperature T_m, which does not vary during the phase transition. In amorphous substances, the phase transition temperature is not constant and the state change occurs within a certain range of temperatures, Figure 4. In simplified terms for a macroscopic description of the numerical model, the phase change of a material is understood as a state in which the material changes its physical characteristics on the basis of variations (external) of its thermodanymic system. This state is often accompanied by a nonlinear effect, Figure 3. The effect involves energy Q supplied to the thermodynamic system of the material, temperature T, latent energy ΔQ necessary to change the externalmacroscopic state of the material, initial state temperature T_0, phase change temperature T_{m} , and temperature T_e limiting the low-temperature mode.

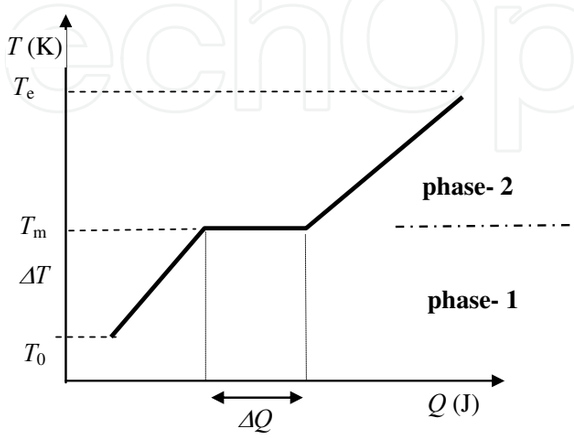

Fig. 3. The PCM macroscopic characteristics

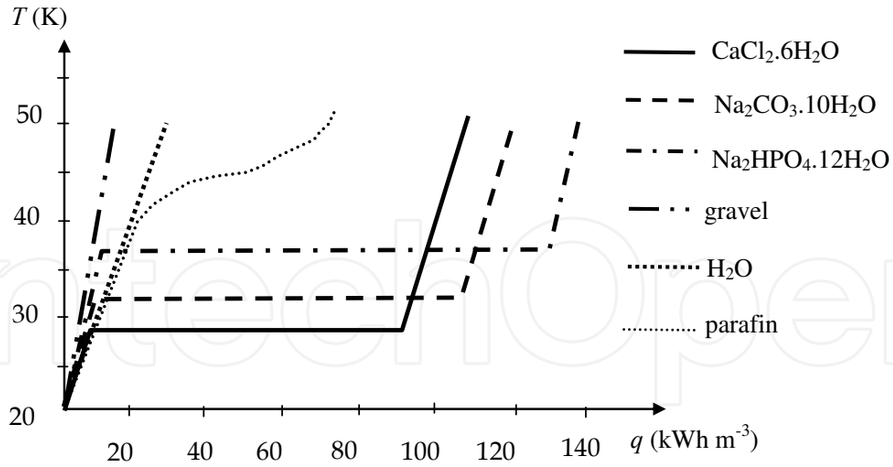

Fig. 4. The course of accumulator charging with PCMs and classical materials

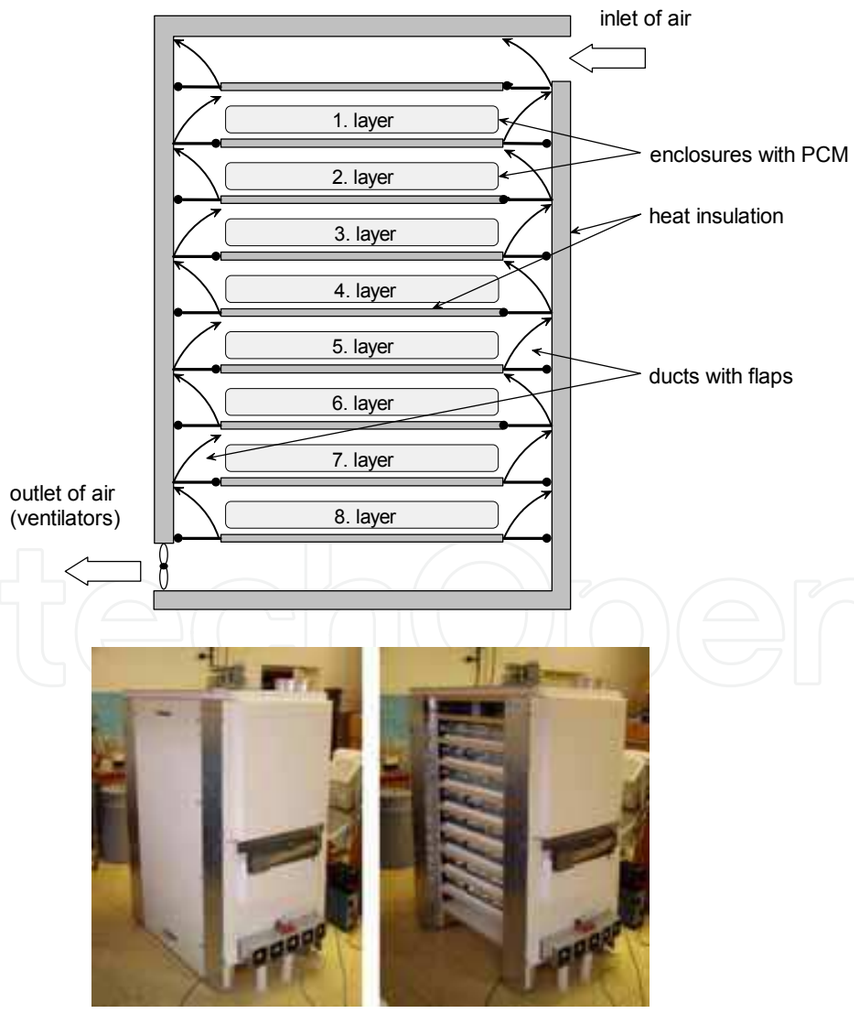

Fig. 5. Experimental model of a heat accumulator

2.5 Requirements placed on the PCM, reservoirs and casings

PCM materials applicable for the accumulation of heat utilizing state change ought to meet the following criteria (Behunek, I. 2002): Physical (a suitable phase diagram in the transition area, a suitable phase transition temperature, small changes of volume during the change of state, high density of the substance, supercooling tolerance, high specific melting heat, good thermal conductivity), chemical (nonflammability, nontoxicity, chemical stability, anticorrosive properties), economical (low asking price, availability, low cost of a suitable accumulator). The structure of PCM reservoirs must conform to standard requirements placed on thermal containers. In general, with respect to the provision of a suitable speed of heat transfer, it is necessary to encase the actual PCM material and insert the resulting containers that hold the PCM into an external envelope; this insertion should be realized in such a way that, through its circulation, the heating medium ensures an optimum transfer of heat energy in both directions (during charging and discharging), Figure 5.

Consequently, there exists substantial similarity to caloric reservoirs containing crushed stone (aggregate) and therefore the rules governing the construction of these reservoirs can be applied.

2.6 Basic classification of PCM materials

If we are to futher consider the properties of PCMs, it is necessary to describe their minimum classicification and properties in phase changes, relation (3).

a. The advantages of *anorganic substances* (GARG, H.P. et al. 1985, VENER, C. 1997) mainly consist in the high value of specific melting heat, good thermal conductivity, nonflammability, and low cost. The negative characteristics include corrosivity of the substances to most metals, decomposition, loss of hygroscopic water, and the possibility of supercooling.

Examples of anorganic PCMs are as follows:
$CaCl_2.6H_2O$, $Na_2SO_4.10H_2O$, $Na_2CO_3.10H_2O$, $MgCl_2.6H_2O$, $CaBr_2.6H_2O$, $Mg(NO_3)_2.6H_2O$, $LiNO_3.3H_2O$, $KF.4H_2O$, $Na_2SO_4.10H_2O$, $Na_2HPO_4.12H_2O$.

$$X(Y)_n \cdot mH_2O \xleftrightarrow{\text{teplo}} X(Y)_n \cdot pH_2O + (m-p)H_2O \tag{3}$$

b. *Organic substances* (GARG, H.P. et al. 1985, VENER, C. 1997) offer advantages such as a high value of specific melting heat, chemical stability, elimination of supercooling, and no corrosivity. The disadvantages consist in the inferior thermal conductivity, relatively significant variations of volume during the change of state, flammability). Examples of organic PCMs include paraffin, wax, polyethylene glycol, high-density polyethylene, stearic acid ($C_{17}H_{35}COOH$), and palmitic acid ($C_{15}H_{31}COOH$).
c. *Other substances* include compounds, combinations of amorphous and crystalline substances, kombinace amorfních a krystalických látek, clathrates, and other items.

The advantage of low-potential heat accumulation in PCM application consists in the variability. A comparison of PCM and classical materials together with a listing of several PCMs (] LANE, G.A. 1983, FAVIER, A. 1999) is provided in Table 1. The elementary reference quantity is the density of accumulated energy. We assume the initial charging temperature as T_0 20 °C and the final termperature as T_e 50 °C. The course of accumulator loading with various types of filling (charge) is shown in Figure 4; a realization example of a PCM-based accumulator is provided in Figure 5.

Material used for accumulation in heat reservoir	Accumulated energy density q [kWh.m^{-3}]
Water	34,5
Aggregate of stones	23,0
Paraffin	62,4
$CaCl_2$. $6H_2O$	117,4
Na_2CO_3 . $10H_2O$	131,7
Na_2HPO_4 . $12H_2O$	134,7

Table 1. A comparison of accumulated energy density for different substances

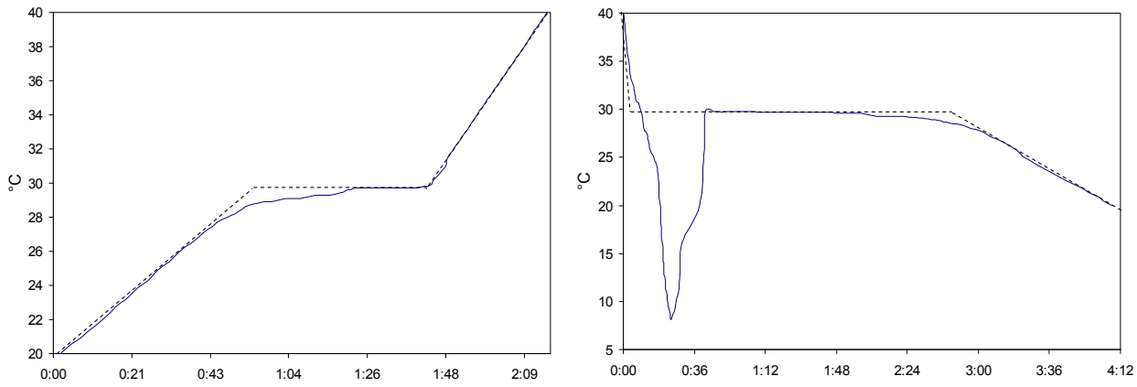

Fig. 6. Phase changes of $CaCl_2.6H_2O$

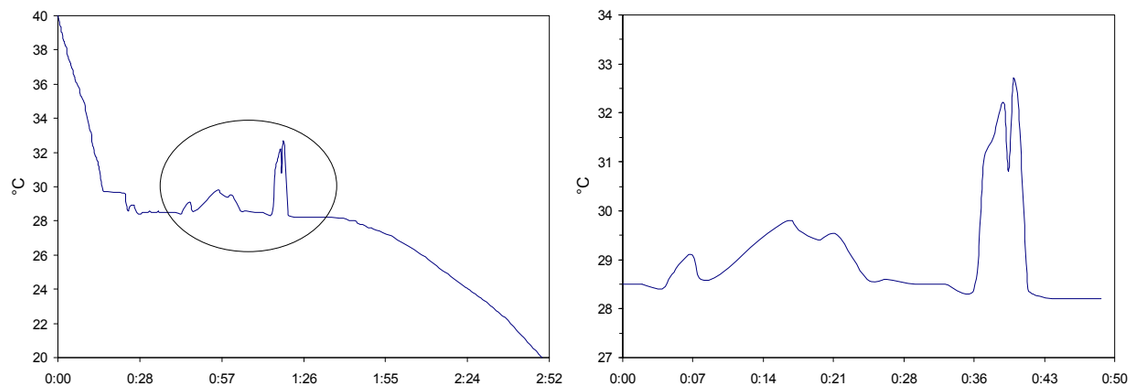

Fig. 7. Phase change of $CaCl_2.6H_2O$ ($CaCl_2.4H_2O$ crystallization)

2.7 Calcium chloride hexahydrate and its modification

In Figure 6, the phase change of $CaCl_2.6H_2O$ during heating and cooling is shown. The dashed lines show the theoretical behaviour under the condition when the melting and freezing were realized at constant temperature T_m – the case of pure crystallic substances. Impurity and the methodology of measuring are the main cause of variations (the probe has to be placed only in small amounts of hexahydrate. During solidification, ing occurred

owing to weak nucleation. Crystallization was initiated thanks to a solid particle of the PCM added to the measured sample. Otherwise, the crystallization would not have occurred. The group of materials for the encasing of hexahydrate may include plastics, mild steel or copper; aluminium or stainless steel are not suitable.
In some cases, temperature fluctuation above T_m may occur during solidification (Figure 7). The explanation was found in the binary diagram.
Figure 4 indicates the binary phase diagram of calcium chloride and water. The hexahydrate contains 50,66 wt% $CaCl_2$, and the tetrahydrate 60,63 wt%. The melting point of the hexahydrate is 29,6 °C, with that of the tetrahydrate being 45,3 °C. The hexahydrate-α tetrahydrate peritectic point is at 49,62 wt% $CaCl_2$-50,38 wt% H_2O, and 29,45 °C. In addition to the stable form, there are two monotropic polymorphs of the tetrahydrate salt, β and γ. The latter two are rarely encountered when dealing with the hexahydrate composition; however, the α tetrahydrate is stable from its liquidus temperature, 32,78 °C, down to the peritectic point, 29,45 °C, thus showing a span of 3,33 °C. When liquid $CaCl_6.6H_2O$ is cooled at the equilibrium, $CaCl_2.4H_2O$ can begin to crystallize at 32,78 °C. When the peritectic is reached at 29,45 °C, the tetrahydrate hydrates further to form hexahydrate, and the material freezes. The maximum amount of tetrahydrate which can be formed is 9,45 wt%, calculated by the lever rule. This process is reversed when solid $CaCl_6.6H_2O$ is heated at the equilibrium. At 29,45 °C the peritectic reaction occurs, forming 9,45% of $CaCl_2.4H_2O$ and the liquid of the peritectic composition. With increasing temperature, the tetrahydrate melts, disappearing completely at 32,78 °C. Under actual freezing and melting conditions, the equilibrium processes described above may occur only partially or not at all. Supercooling of the tetrahydrate may lead to initial crystallization of the hexahydrate at 29,6 °C (or lower if this phase also supercools). It is possible to conduct modification by additives. From a number of potential candidates, $Ba(OH)_2$, $BaCO_3$ and $Sr(OH)_2$ were chosen as they seemed to be feasible. When we used $Ba(OH)_2$ and $Sr(OH)_2$ at 1% part by weight, there was no supercooling. We were able to increase the stability of the equilibrium condition by adding KCl (2 wt%) and NaCl, Figure 8. NaCl is a weak soluble in $CaCl_2.6H_2O$, therefore the part by weight is only about 0,5%. The related disadvantage is that the melting point decreases by ca. 3 °C at 26-27 °C.

2.8 Numerical model of heat accumulators

The effectivity of transferring the heat to active elements in the accumulator consists in the optimum setting of dimensions and shapes in the process of circulation of the medium that transfers energy in the accumulator. Therefore, a necessary precondition of the design consisted in solving the air circulation model under the condition of change in its temperature and thermodynamical variations in the PCM material. The actual model of active elements and its temperature characteristic is not fundamental to this task; the characteristic is known and realizable through commonly appplied methods.
A geometric model of one layer of the accumulator is shown in Figure 10 (Behunek, I. 2004) It consists of 26 PVC pipes in a square configuration (Lienhard, J.H. IV & Lienhard, J.H. V. 2004). Inside of the pipes there are 9,36 litres of modified $CaCl_2.6H_2O$. The air flows through the layer and transfers heat into the pipes. The related numerical solution was realized in two parts. First, we solved the turbulence model and obtained the heat transfer film coefficients. These results constituted the input for the solution of the second part namely the calculation of the thermal model. The time dependence of temperature distribution in the layer is the final result.

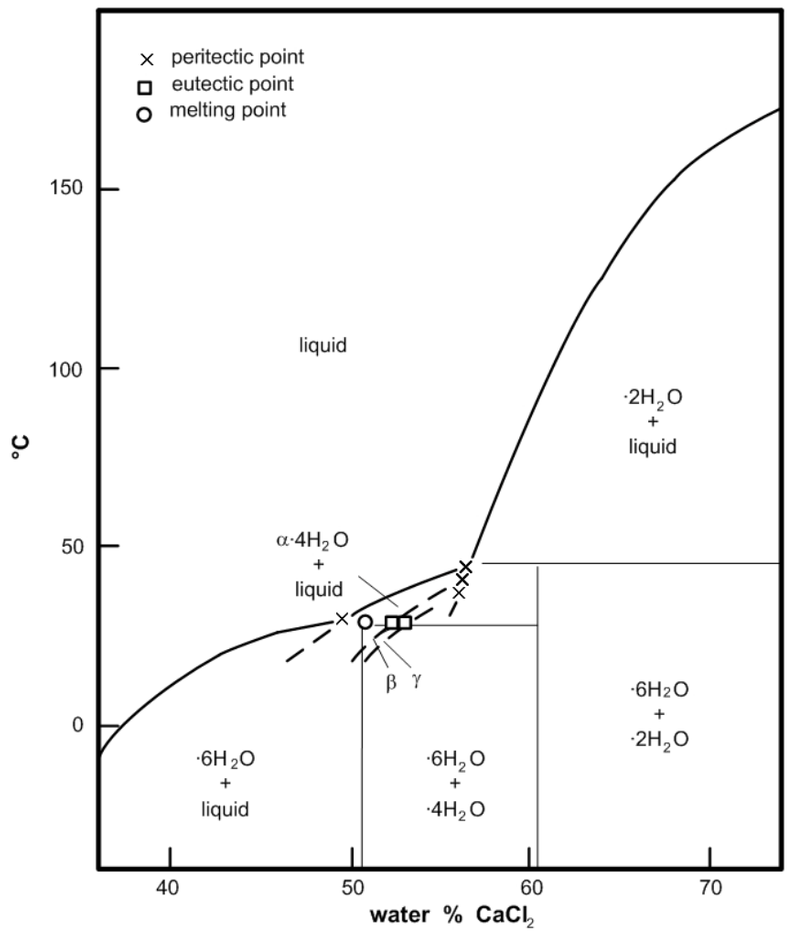

Fig. 8. Binary diagram of $CaCl_2.6H_2O$ [9]

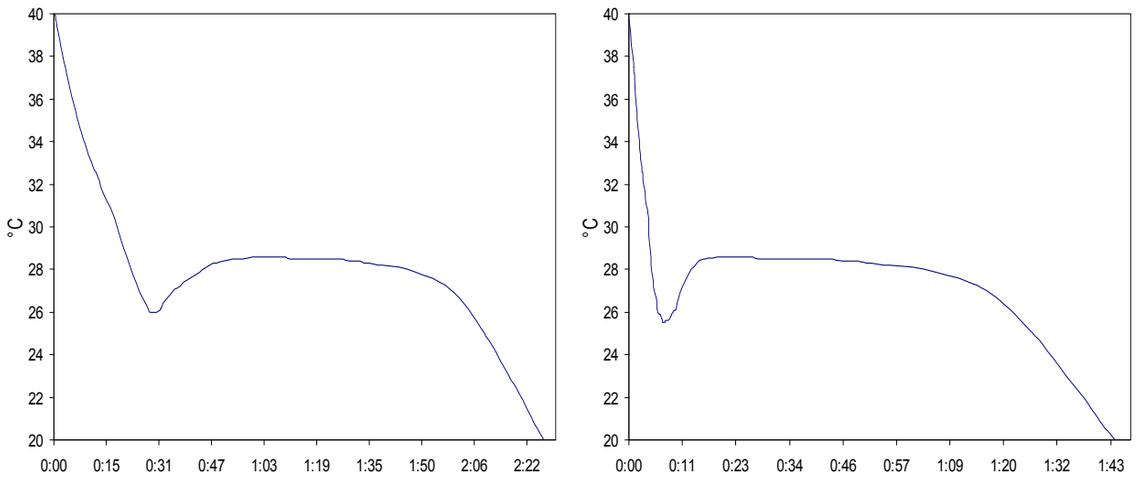

Fig. 9. Modification of $CaCl_2.6H_2O$ at a different rate of heat removal

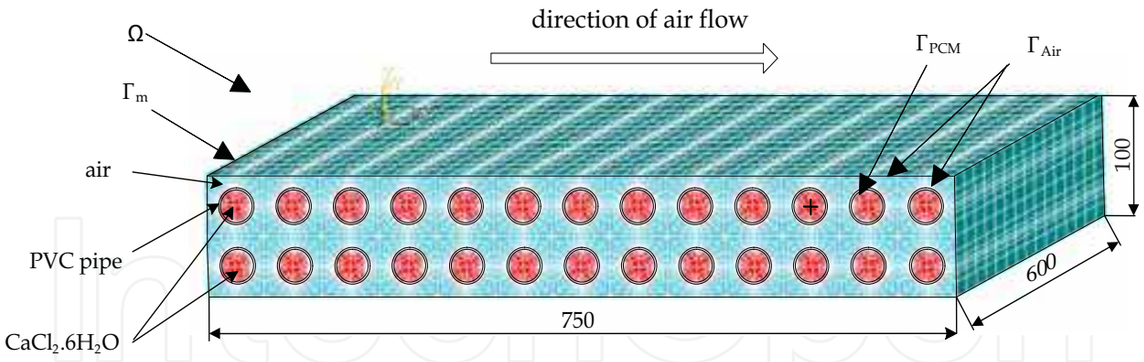

Fig. 10. Geometric model of a layer with the mesh of elements

2.8.1 Mathematical and numerical model

The mathematical model of air velocity distribution uses fluid equations which were derived for the incompressible fluid with the condition

$$div\ \nu = 0 \tag{4}$$

For a steady state of flow there holds the continuity equation

$$div\ \rho\nu = 0 \tag{5}$$

We assume a turbulent flow

$$curl\ \nu = 2w \tag{6}$$

where $\boldsymbol{\omega}$ is the angular velocity of fluid. If we use the Stokes theorem, the Helmholtz theorem for the moving particle and the continuity equation, we can formulate from the equilibrium of forces the Navier-Stokes equation for the fluid element

$$\frac{\partial \boldsymbol{v}}{\partial t} + (grad\boldsymbol{v})\cdot\boldsymbol{v}^T = \boldsymbol{A} - \frac{1}{\rho} grad\, p + \boldsymbol{\upsilon}\cdot\Delta\boldsymbol{v} \tag{7}$$

where $\boldsymbol{A}$ is the external acceleration, $\boldsymbol{\upsilon}$ the vector of kinematic viscosity, and ($grad\ \boldsymbol{v}$) has the dimension of tensor. In equation (7) we substitute pressure losses

$$\begin{aligned} grad\, p = &-\left(K_x \rho v_x |v| + \frac{f}{D_h}\rho v_x |v| + C_x \mu v_x \right) u_x - \left(K_y \rho v_y |v| + \frac{f}{D_h}\rho v_y |v| + C_y \mu v_y \right) u_y \\ &- \left(K_z \rho v_z |v| + \frac{f}{D_h}\rho v_z |v| + C_z \mu v_z \right) u_z \end{aligned} \tag{8}$$

where K are the suppressed pressure losses, f the resistance coefficient, D_h the hydraulic diameter of ribs, C the air permeability of system, μ the dynamic viscosity, and $\boldsymbol{u}_{x,y,z}$ the unit vector of the Cartesian coordinate system. The resistance coefficient is obtained from the Boussinesq theorem

$$f = aRe^{-b} \tag{9}$$

where *Re* is Reynolds number and *a*, *b* are coefficients from [40]. The model of short deformation field is formulated from the condition of steady-state stability, which is expressed

$$\int_{\Omega} \boldsymbol{f}\,\mathrm{d}\Omega + \int \boldsymbol{t}\,\mathrm{d}\Gamma = 0 \tag{10}$$

where $\boldsymbol{f}$ are the specific forces in domain $\boldsymbol{\Omega}$, and $\boldsymbol{t}$ the pressures, tensions and shear stresses on the interface area $\boldsymbol{\Gamma}$. By means of the transformation into local coordinates, we obtain the differential form for the static equilibrium

$$\boldsymbol{f} + div^2 \boldsymbol{T}_{\mathrm{v}} = 0 \tag{11}$$

where div^2 stands for the div operator of tensor quantity and $\boldsymbol{T}_{\mathrm{v}}$ is the tensor of internal tension

$$\boldsymbol{T}_{\mathrm{v}} = \begin{bmatrix} X_{\mathrm{x}} & X_{\mathrm{y}} & X_{\mathrm{z}} \\ Y_{\mathrm{x}} & Y_{\mathrm{y}} & Y_{\mathrm{z}} \\ Z_{\mathrm{x}} & Z_{\mathrm{y}} & Z_{\mathrm{z}} \end{bmatrix} \tag{12}$$

where *X*, *Y*, *Z* are the stress components which act on elements of the area. It is possible to add a form of specific force from (4)-(7) to the condition of static equilibrium. The form of specific force is obtained by means of an external acceleration $\boldsymbol{A}$, on the condition that pressure losses and shear stresses τ are given as

$$\rho\left(\frac{\partial \boldsymbol{v}}{\partial t} + \cdot(grad\boldsymbol{v})\cdot \boldsymbol{v}^{T}\right) - \rho\boldsymbol{A} - \sum_{l=1}^{N_{\mathrm{s}}} \boldsymbol{F}_{\mathrm{l}} + div^2 \boldsymbol{T}_{\mathrm{v}} = \boldsymbol{0} \tag{13}$$

where $\boldsymbol{F}_{\mathrm{l}}$ are the discrete forces and div^2 is the divergence operator of tensor. The model which covers the forces, viscosity, and pressure losses is

$$\rho\left(\frac{\partial \mathrm{v}}{\partial t} + \cdot\left(grad\,\mathrm{v}\right)\cdot \mathrm{v}^{T}\right) - \rho\mathrm{A} - \sum_{l=1}^{N_{\mathrm{s}}} \mathrm{F}_{\mathrm{l}} + grad\,p - \mu\cdot\Delta\,\mathrm{v} = 0 \tag{14}$$

We can prepare the discretization of equation (7) by means of the approximation of velocity $\boldsymbol{v}$ and acceleration $\boldsymbol{a}$ (Behunek I, Fiala P. Jun 2007). On the interface there are defined boundary and initial conditions. Initial and boundary conditions can be written; the initial temperature of the air is 50 °C, the initial velocity of the air is 0,4 m.s^{-1}, the outlet pressure is 101,3 kPa + 10 Pa, and the initial temperature of the air inside the accumulator, PVC and $CaCl_2.6H_2O$ is 20 °C. There are the distribution of velocity values indicated in figures 11, 12, and other results for the distribution of turbulent kinetic energy, dissipation, temperature and pressure follow on Figures 13. Calculation of the thermal model (finite element methode (FEM), finite volume methode (FVM), Ansys User's Manual) was realized under the same conditions as the previous turbulence model.

Figure 13 shows the time dependence of temperature in $CaCl_2.6H_2O$ in the pipe marked with a black cross (Figure 11). We can compare the result of the numerical simulation with the measurement. Differences between the simulation and the measurement are caused by the inaccuracy of the model with respect to reality.

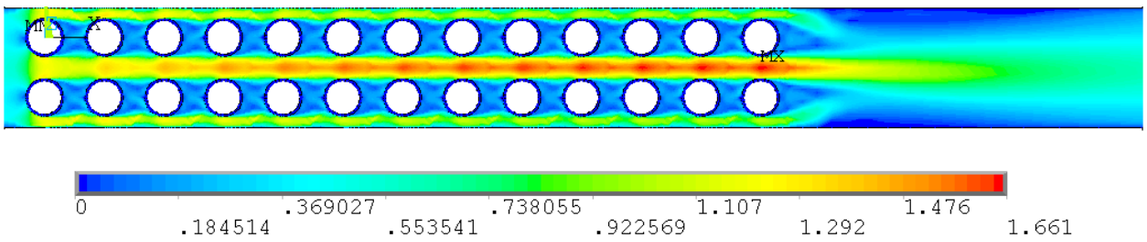

Fig. 11. Velocity distribution of the air

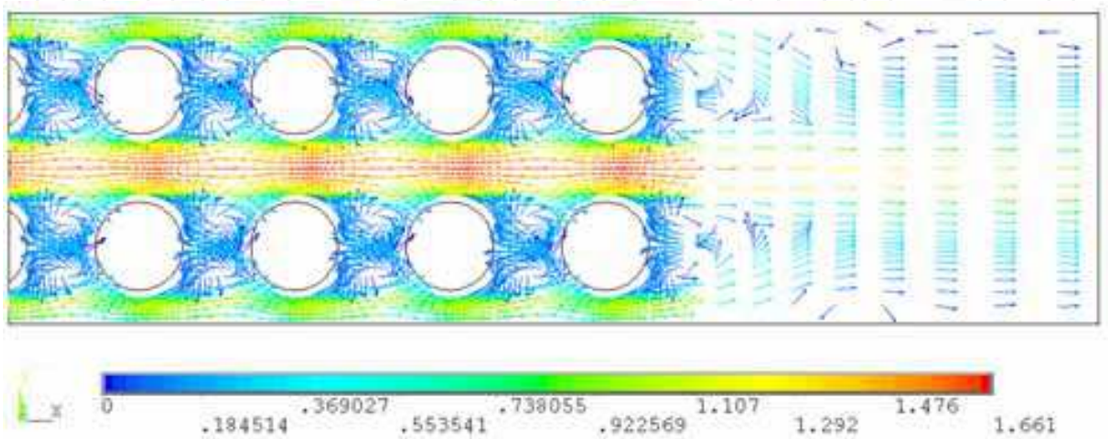

Fig. 12. Velocity distribution of the air (vectors, detail)

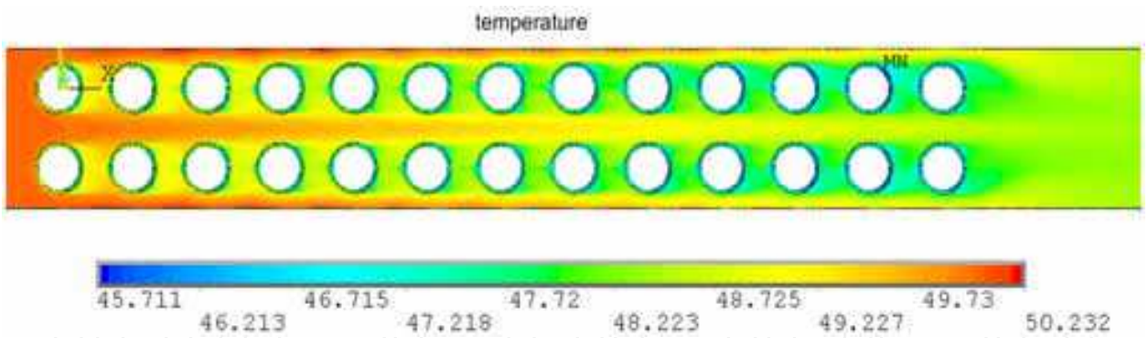

Fig. 13. Distribution of temperature

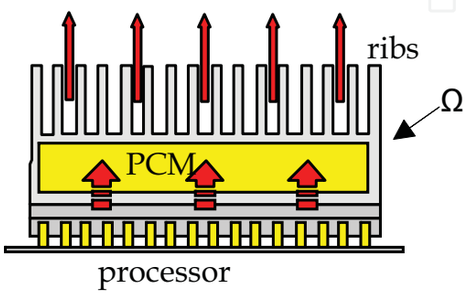

Fig. 14. Example of a processor cooler with a phase change material)

We used tabular values of pure $CaCl_2.6H_2O$; howerer, the pipes contain modified hexahydrate with 1,2% of $BaCO_3$.

3. Cooling system

The PCM may be used for active or passive electronic cooling applications with high power at the package level (see Figure 14).

3.1 Analytical description and solution of heat transfer and phase change

We analyze the problem of heat transfer in a 1D body during the melting and freezing process with an external heat flux or heat convection, which is given by boundary conditions. The solution of this problem is known for the solidification of metals. We tried to apply this theory to the melting of crystalline salts. The 1D body could be a semifinite plane, cylinder or sphere. As the solid and the liquid part of PCM have different temperatures, there occurs heat transfer on the interface. According to Fig. 16, the origin of x is the axis of pipe, centre of sphere, or the origin of plate. Liquid starts to solidify if the surface is cooled by the flowing fluid ($T_w < T_m$). The equation describing the solid state is

$$\frac{\partial T_s}{\partial t} = \frac{a_s}{x^n}\frac{\partial}{\partial x}\left(x^n \frac{\partial T_s}{\partial x}\right) \tag{15}$$

where for the plate $n = 0$, cylinder $n = 1$ and sphere $n = 2$; a_s is the thermal diffusion coefficient in the solid state. For $x = x_0$ we can assume the following boundary conditions: constant temperature

$$T = T_w \tag{16}$$

or constant heat flux

$$\lambda_s \frac{\partial T_s}{\partial x} = -q_w \tag{17}$$

or for convective cooling

$$\lambda_s = \frac{\partial T_s}{\partial x} = -k(T - T_b) \tag{18}$$

where q_w is the specific heat flux and λ_s is the thermal conductivity coefficient. Initial condition ($t = 0$) for (24) is

$$T_s(0) = T_0. \tag{19}$$

For the interface between the solid and the liquid we obtain

$$\rho_s \Delta h_m \frac{ds}{dt} = \lambda_s \frac{\partial T_s}{\partial x} + \alpha(T_m - T_0). \tag{20}$$

The analytical solution is exact but we consider several simplifying assumptions. The most important of these is that we can solve the solidification of PCM only in a one-dimensional body.

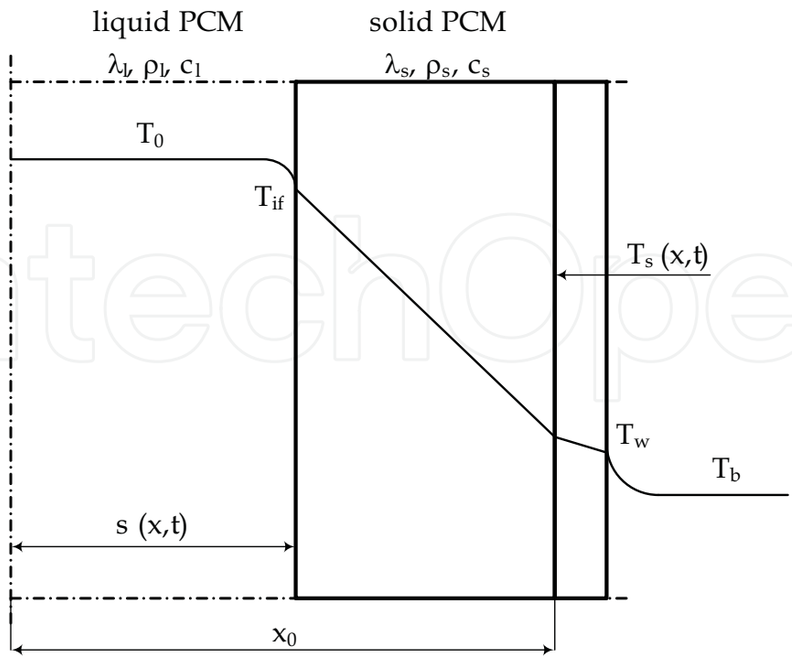

Fig. 15. Heat transfer on the interface between the solid and the liquid parts

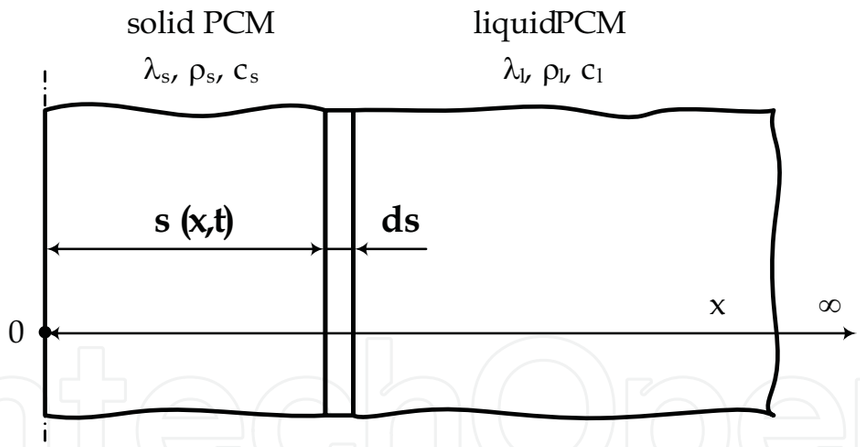

Fig. 16. Solidification of a semi-infinite plate of PCM

We consider a semi-infinite mass of liquid PCM at initial temperature T_0, which was cooled by a sudden drop of surface temperature T_p = 0 °C. This temperature is constant during the whole process of solidification. The simplifying assumptions are as follows: The body is a semi-infinite plane, the heat flux is one-dimensional in the x-axis, the interface between the solid and the liquid is planar, there is an ideal contact on the interface, the temperature of the surface is constant (T_p = 0 °C), the crystallization of PCM is at a constant temperature T_m, the thermophysical properties of the solid and the liquid are different but independent of the temperature, there is no natural convection in the liquid. The initial and boundary conditions involve initial temperature T_0 for $x \geq 0$ at time 0; the temperature equals T_m on the interface between the solid and the liquid ($x = s$)

$$x = s \wedge t > 0 \quad \Rightarrow \quad T_s = T_l = T_m = const \tag{21}$$

The evolved latent heat during the interface motion (the thickness of volume element *ds*, area 1 m², time 1 s) is

$$dQ_{\Delta h_m} = \Delta h_m \rho_l 1 \frac{ds}{dt} \tag{22}$$

Position of the interface is a function of time

$$s = s(t) = 2\varepsilon\sqrt{a_s t}, \tag{23}$$

This dependence is called the parabolic law of solidification, where ε is the root of equation describing the freezing. The boundary and initial condition for the phase change is

$$\lambda_s \left(\frac{\partial T_s}{\partial x} \right)_{x=s} = \lambda_l \left(\frac{\partial T_l}{\partial x} \right)_{x=s} + \Delta h_m \rho_l \frac{ds}{dt} \tag{24}$$

$$x \to \infty \wedge t > 0 \quad \Rightarrow \quad T_l = T_0 = const \tag{25}$$

$$x = 0 \wedge t \geq 0 \quad \Rightarrow \quad T_p = T_s(x = 0) = 0\ ^\circ\mathrm{C} \tag{26}$$

If we solve the Fourier relations of heat conduction under the above-given conditions for the solid and the liquid, we get the equations below which allow for the calculation of temperatures in the solid, liquid PCMs as well as the location of interface. The results are shown in Figure 17, (Behunek I & Fiala P. Jun 2007).

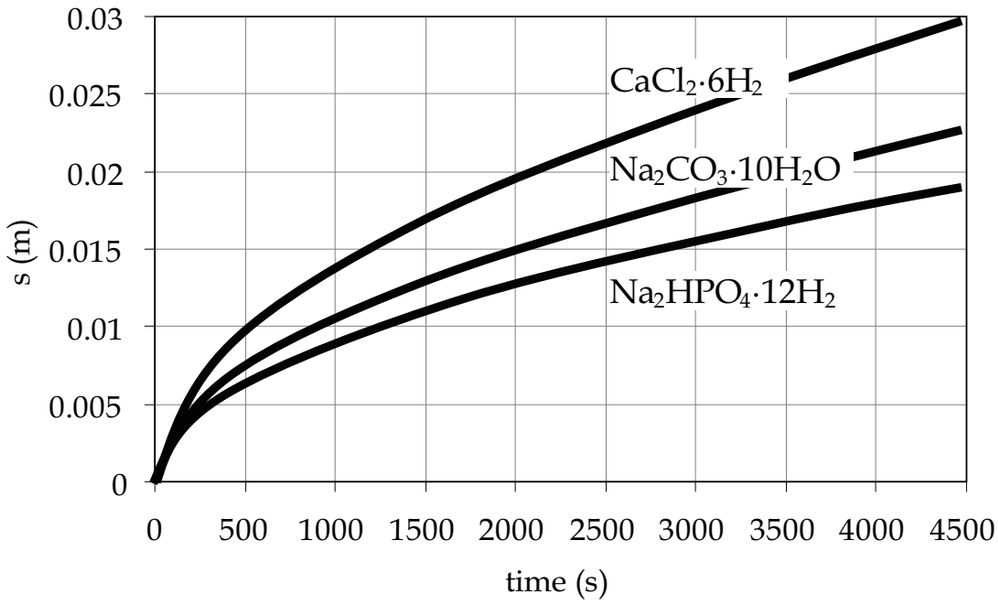

Fig. 17. Position between the solid and the liquid PCM

3.2 Nymerical analysis of heat transfer and phase change

If we compare the results of the analytical solution with the experimental measurement of the materials (Behunek, I. 2002), we can see a good agreement. Outside domain Ω, is the air velocity and pressure are zero. We can write the form for an element of mesh related to the (Behunek I & Fiala P. Jun 2007) Cu-cooler with PCM. For the description of different turbulent models see (Piszachich, W.S. 1985, Wilcox, D.C. 1994). The numerical solution consists of two parts. Firstly, we solve the turbulence model and obtain heat transfer coefficients on the surface of the ribs. These results constitute the input for the second part, in which the thermal model is calculated. We obtain the time dependence of temperature distribution in the PCM. A geometric model of a copper cooler in shown in Figure 19. The $CaCl_2.6H_2O$ is closed inside of the bottom plate (see Figure 14). The size of the plate is 30x30x5 mm, and the ribs are 20 mm in height. The PCM volume is approximately $3{,}8.10^{-6}$ m^3. The plate takes the heat from the processor up and the crystalline salt starts to melt at T_m. The air flows through the ribs and extracts heat from the cooler. In Figure 20, the distribution of air velocity module is indicated. We can see the effective rise of air flow velocity at the bottom of the ribs (detail A in Figures 19, 20). Temperature distribution in the ribs is shown in Figure 20, Figure 21 compares the results of numerical simulation with the measuring in the middle of PCM enclosure (casing). We measured the temperature by means of a probe.

The differences between the simulation and the measurement are due to the inaccuracy of the model with respect to reality. We used tabular values of pure $CaCl_2.6H_2O$ but we modified the hexahydrate with 1,2% of $BaCO_3$. to avoid supercooling and deformation of cooling curves after more cycles of melting and freezing. In order to obtain exact results, we would nevertheless need to obtain exact knowledge of the temperature dependence of thermal conductivity, specific heat and density during phase change (see Figure 22).

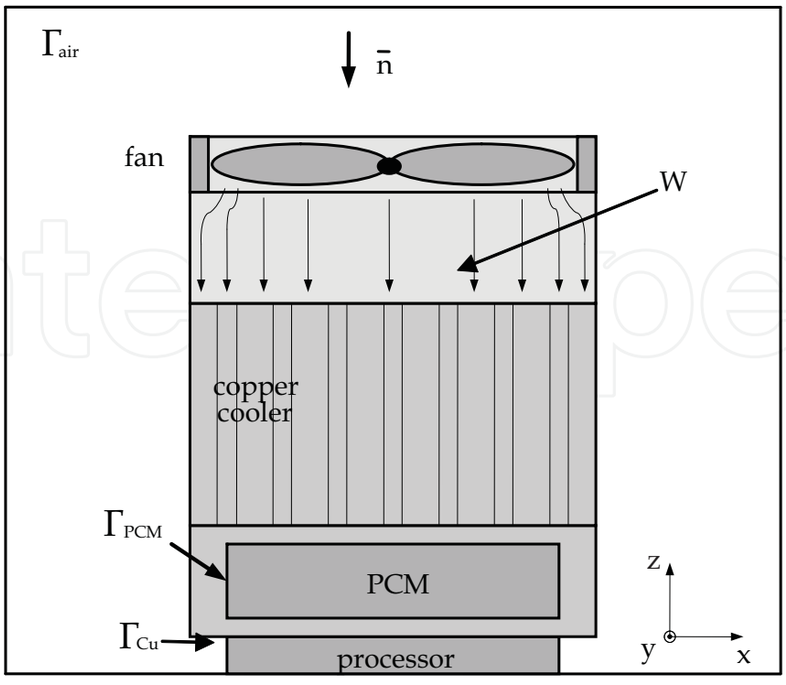

Fig. 18. Geometric model of a Cu-cooler with PCM elements

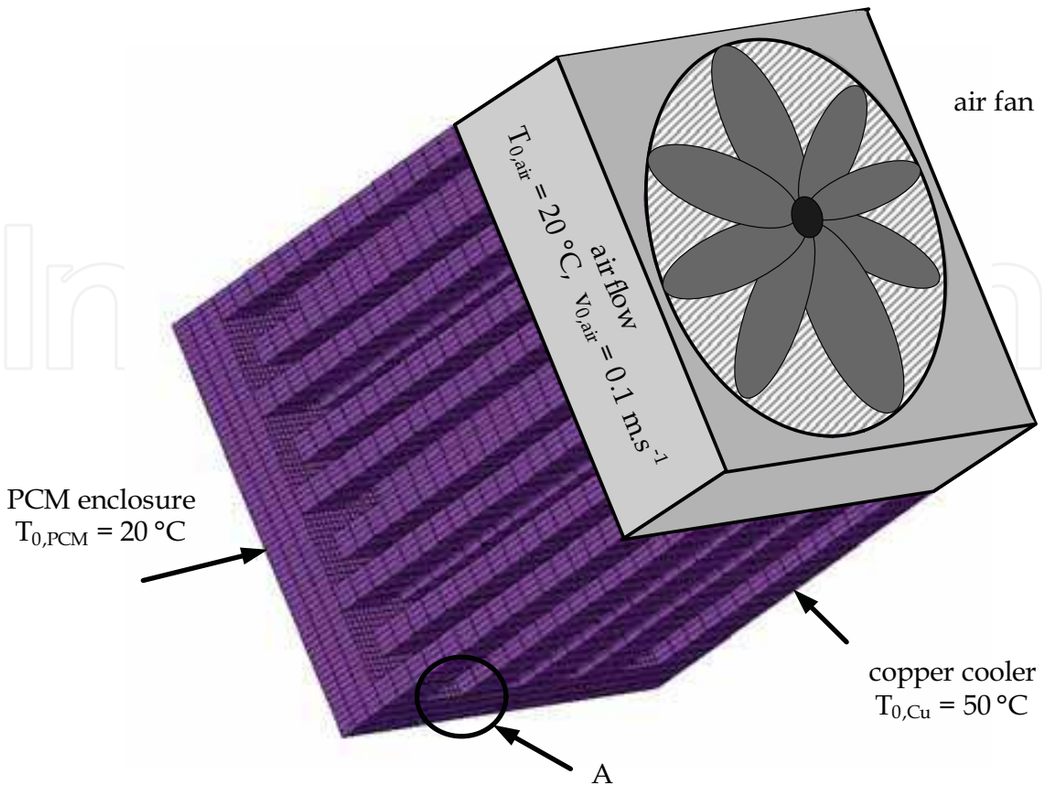

Fig. 19. Geometric model of a Cu-cooler with the mesh of elements

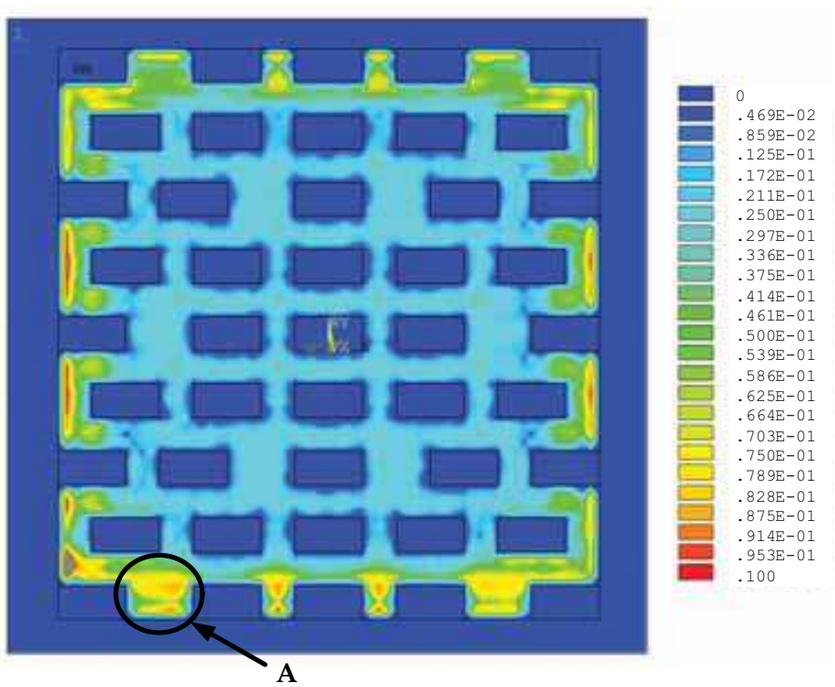

Fig. 20. The distribution of air velocity module

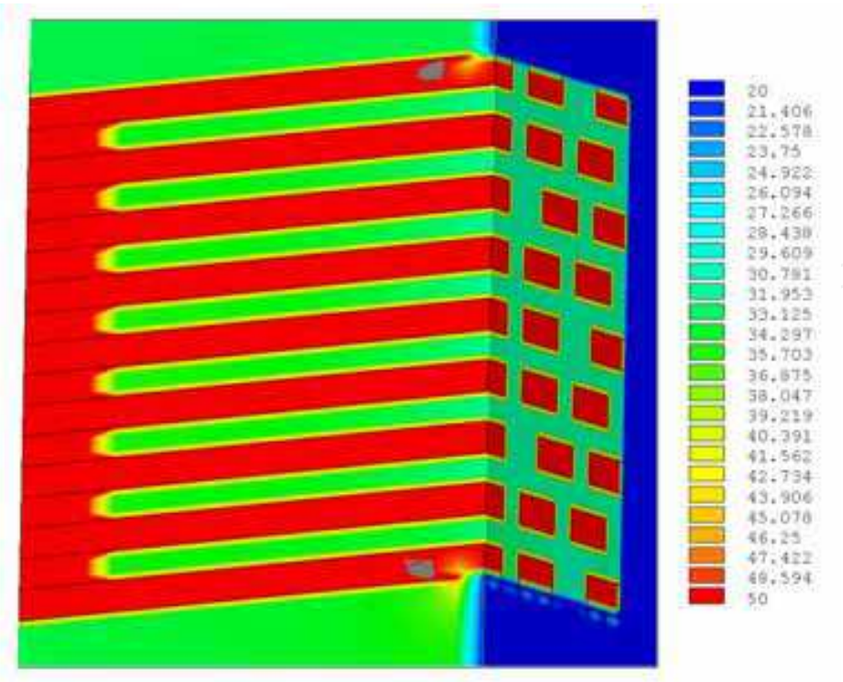

Fig. 21. Temperature distribution in the cooler (the cross section)

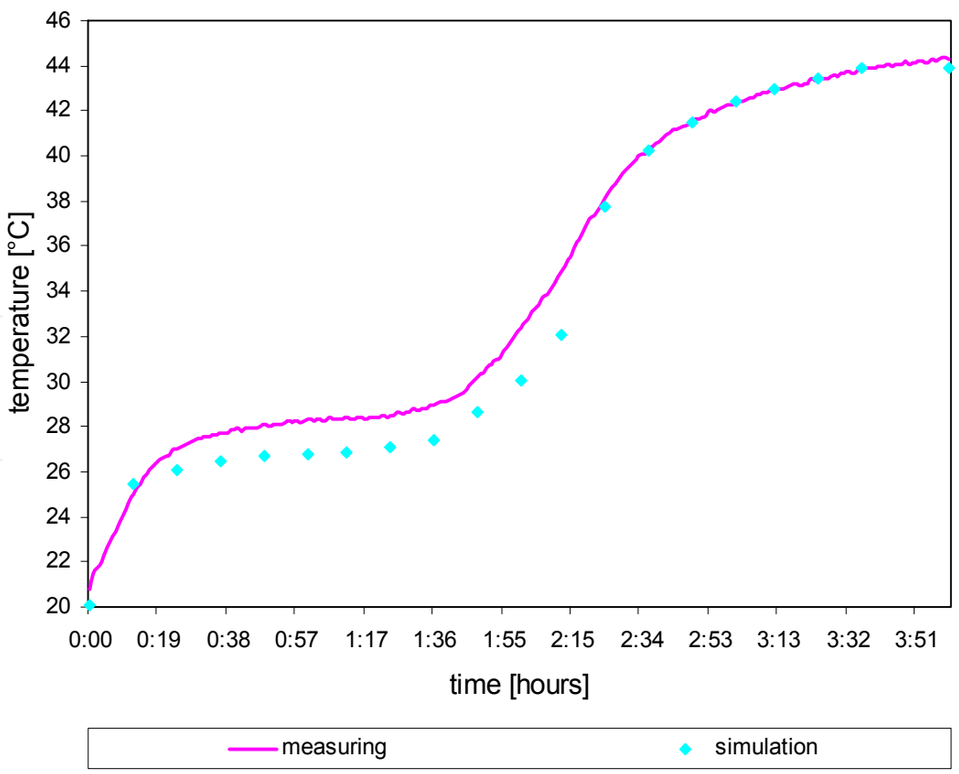

Fig. 22. Comparison between the measurement and the simulation

3.3 Results of the analysis related to accumulators and coolers

The part of the analysis of one layer of a heat accumulator which is derived from the gravel accumulator. We used pure $CaCl_2.6H_2O$ with an additional 1,2% of $BaCO_3$ to increase heat capacity and avoid supercooling. The numerical model was solved by the help of the FEM/FVM in ANSYS software (Ansys User's Manual). If we compare the results of the simulation and the experimental measuring, we will obtain comparatively good congruence. Exact knowledge of the material properties has a crucial effect on the accuracy of the numerical model.

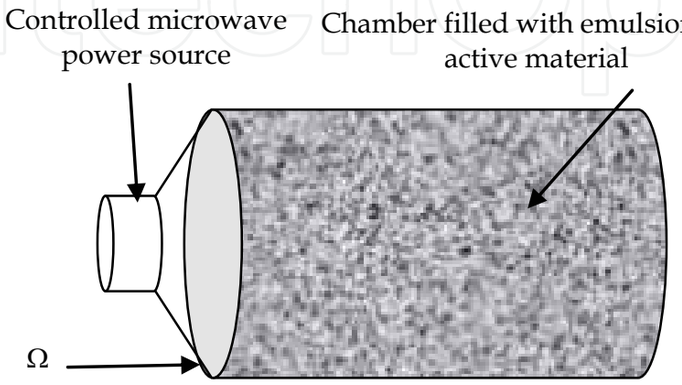

Fig. 23. The basic scheme of the reactor

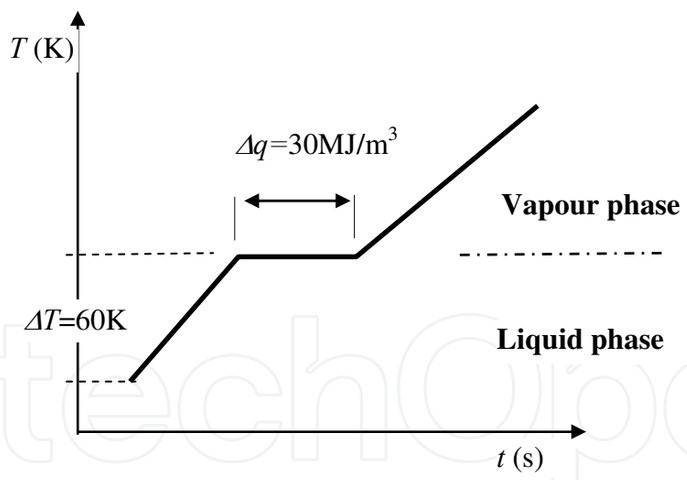

Fig. 24. The phase-change characteristics of water

4. Microwave heating for the separation of the water/oil emulsion

Industrial applications of distribution transformers used in high and mid-performance power distribution systems are supported by maintenance-free systems constructed for the purposes of separation of water bound to the transformer oil. In this case, oil is the insulator whose quality determines the life of the equipment as well as its fault or interference states. The oil is cleaned and filled with adjectives to be reused in functional parts of the transformer, and the related steps are realized in the course of the machine operation. The

described separators may utilize classical properties of H_2O and oil (the mechanical – fluid separation); alternatively, the access of heating or, for example, microwave heating may be applied. In order to use this variant, however, we need to know the process of the material phase change- H_2O to vapour (steam), and the related diversion of the vapour from the separator. Here, the numerical model proved to be superior to all experiments as it enabled us to examine the details of behaviour and states within individual operating modes of the separator. By means of this method, it is possible to model various states of the emulsion as well as fault conditions in the apparatus; thus, we may identify critical sections of the separator design and perform sensitivity analysis of the system. The reactor exploiting active porous substances was designed to enable oil preparation. The reactor is fed with an industrially produced mixture of oil and water; the desired reaction proceeds in the ceramic porous material. To achieve the desired reaction condition, it is necessary to heat the material and, simultaneously, remove the products of the reaction. After the reaction of water, further heating is undesirable with respect to side reactions. Considering the above mentioned requirements, microwave heating was chosen. The microwave heating effect is selective for the reaction of water. The designed reactor operates at the frequency of f = 2.4 GHz, with the magnetron output power of P=800W. This allows selective heating in the active porous material of the chamber. The basic scheme of the reactor is shown in Figure 23.

4.1 Mathematical model

It is possible to carry out an analysis of an MG model as a numerical solution by means of the FEM. The electromagnetic part of the model is based on the solution of full Maxwell's equations

$$\nabla \times \mathrm{E} = -\frac{\partial \mathrm{B}}{\partial t}, \qquad \nabla \times \mathrm{H} = \sigma \mathrm{E} + \frac{\partial \mathrm{D}}{\partial t} + \mathrm{J}_s, \nabla \cdot \mathrm{D} = \rho, \nabla \cdot \mathrm{B} = 0 \quad \text{in region } \Omega. \tag{27}$$

where $\boldsymbol{E}$ and $\boldsymbol{H}$ are the electrical field intensity vector and the magnetic field intensity vector, $\boldsymbol{D}$ a $\boldsymbol{B}$ are the electrical field density vector and the magnetic flux density vector, $\boldsymbol{J}$ is the current density vector of the sources, ρ is the electric charge density, σ is the electric conductivity of the material, and Ω is the definition area of the model. The model is given in manual (Ansys User's Manual). The set of equations (27) is independent of time and gives $\boldsymbol{E}$. For the transient vector $\boldsymbol{E}$ we can write

$$E = \mathrm{Re}\left\{ \underline{E} e^{j\omega t} \right\}. \tag{28}$$

The results were obtained by the solution of the non-linear thermal model with phase change of the medium. The phase change occurs via the phase conversion of water to steam. Figure 28 shows the phase-change time characteristic of water. The thermal model is based on the first thermodynamic law

$$q + \rho \;\; c \;\; \boldsymbol{v} \cdot divT - div\left(k \;\; gradT\right) = \rho c \left(\frac{\partial T}{\partial t} \right), \tag{29}$$

where q is the specific heat, ρ is the specific weight, c is the specific heat capacity, T is the temperature, t is the time, k is the thermal conductivity coefficient, $\boldsymbol{v}$ is the medium flow velocity. If we consider the Snell's principle, the model can be simplified as

$$q - div\left(k \quad gradT\right) = \rho c\left(\frac{\partial T}{\partial t}\right) \tag{30}$$

The solution was obtained by the help of the ANSYS solver. The iteration algorithm (FEM/FVM) was realized using the APDL language as the main program. The simplified description of the algorithm is shown in Figure 25.

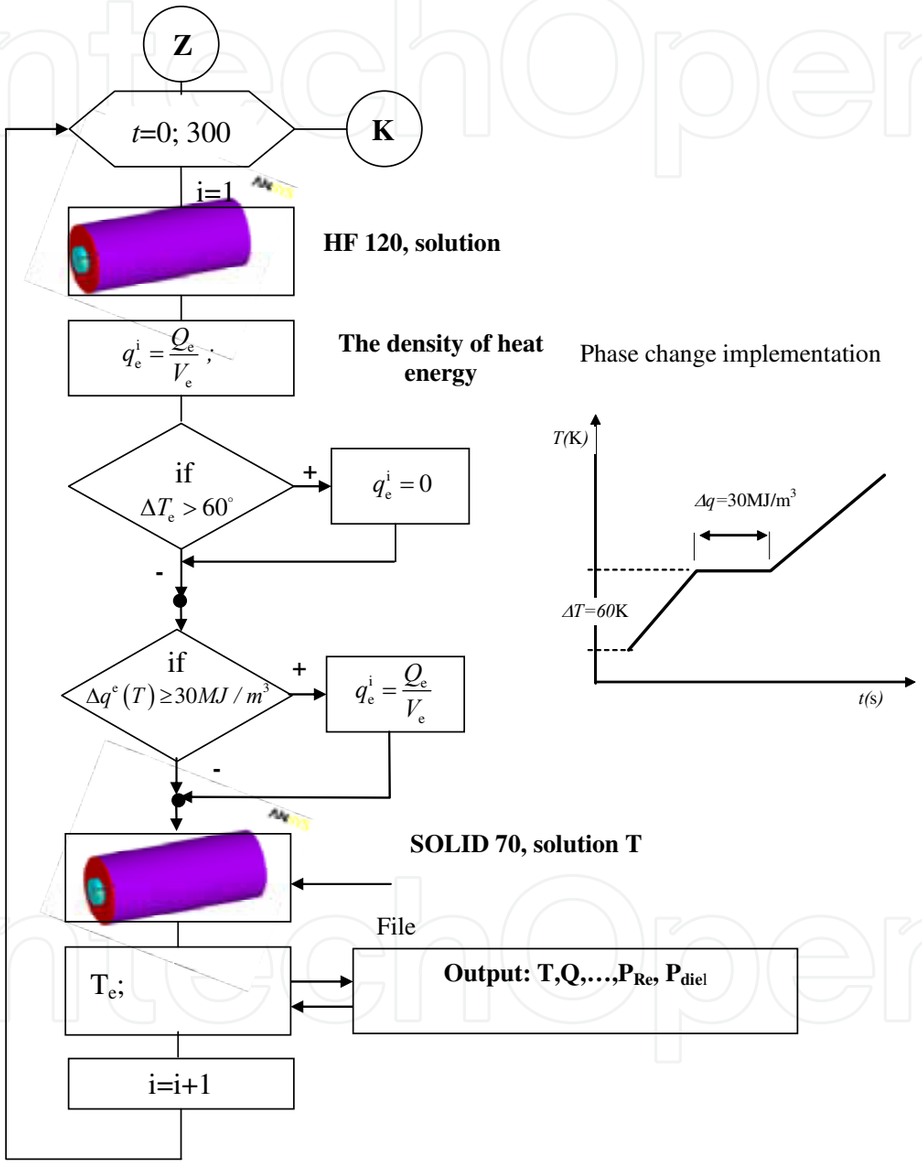

Fig. 25. The simplified iteration algorithm of the model evaluation

4.2 FEM/FVM model

A geometric model using HF119, HF120 and SOLID70 (Ansys User's Manual) in ANSYS software was built – Figure 26. A solution of the coupled field model was performed using the APDL program. The microwave model solution is evaluated according to the specific

heat. The non-linear thermal model including the phase change solves the temperature distribution. The analysis was performed for the time interval $t \in <0,300>$ s and the results were experimentally verified. The simulated results were found to correspond to measured values. A middle electrode was used in the model. The purpose of the middle electrode was to ensure the homogenous distribution of electromagnetic power and, subsequently, to increase the reaction efficiency.

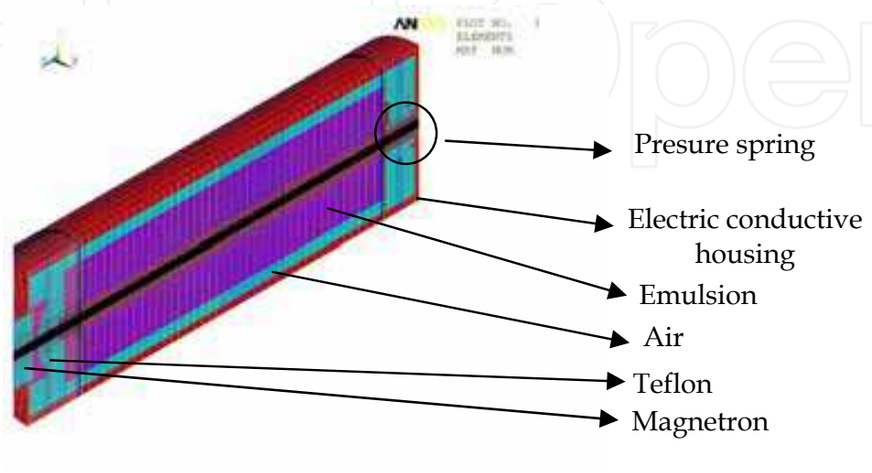

Fig. 26. The geometric model of the HF chamber

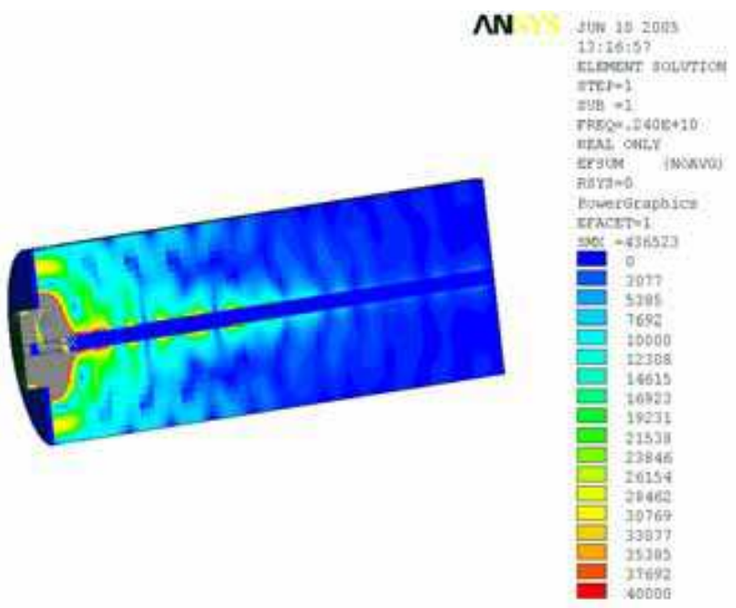

Fig. 27. The distribution of the electric field intensity vector module E

Thesic geometrical model of a separator is shown in Figure. 26; in Figures 26 and 27 we can see the distribution of the electric field vector modules with intensities E as well as the heat generated through the Joule loss in material W_{jh},. Figure 29 shows heating Θ [°C]. In Figure 26, for the given instant of time, the distribution of elements is shown in which phase

change occurred, namely exsiccation and separation of the water from the oil. t=10.8 s, with the magnetron output of P=800W and frequency f=2.4GHz. Figure 31 shows the distribution of temperature rise in the process of exsiccation; here, the indicated aspects include the heat generated through the Joule loss in the material and through dielectric heating for the instant of time t=3.6 s. The distribution of temperature was, for the individual instants, compared with the laboratory measurement.

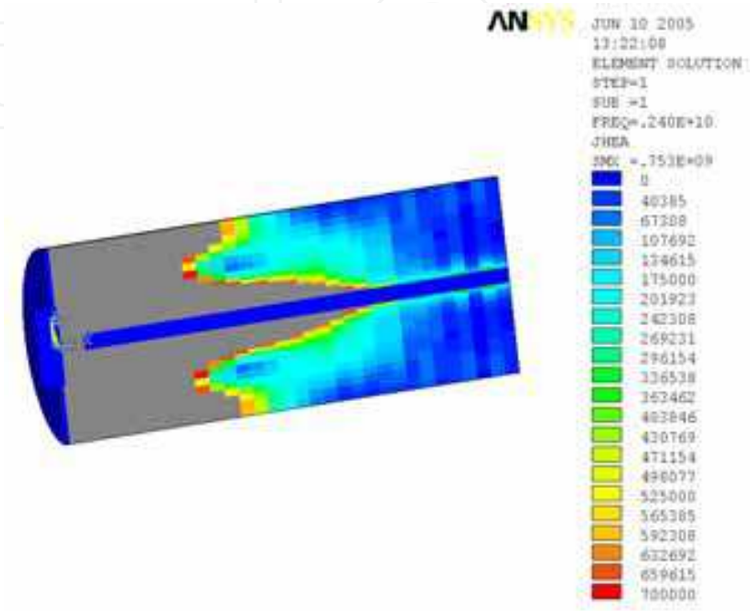

Fig. 28. The distribution module of the Joule heat module W_{jh}

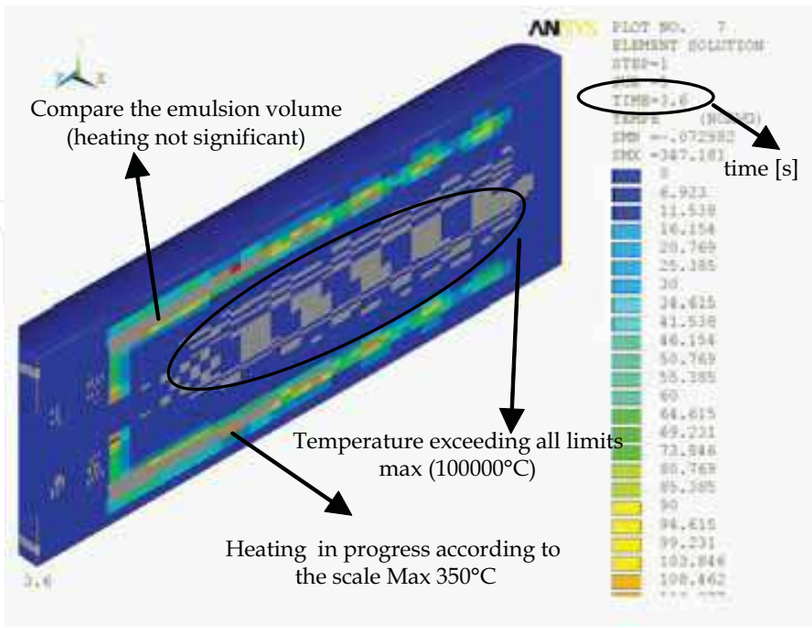

Fig. 29. The distribution of temperature rise Θ

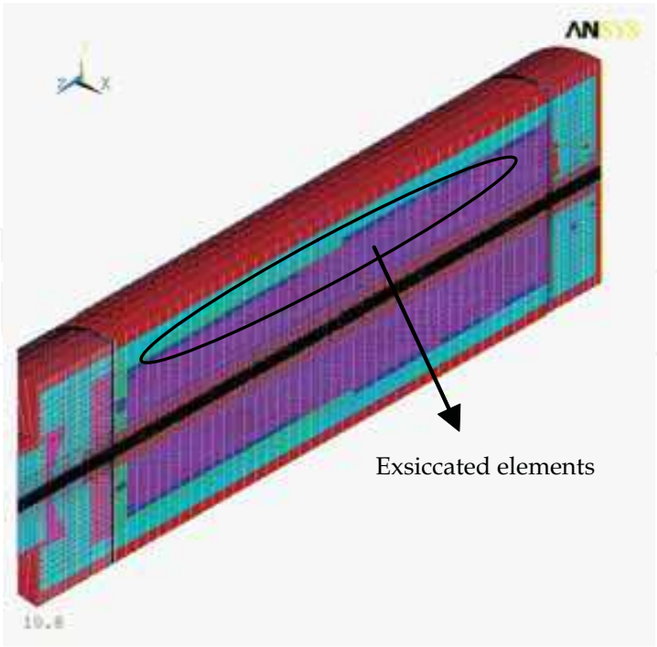

Fig. 30. The emulsion exsiccation process depending on time

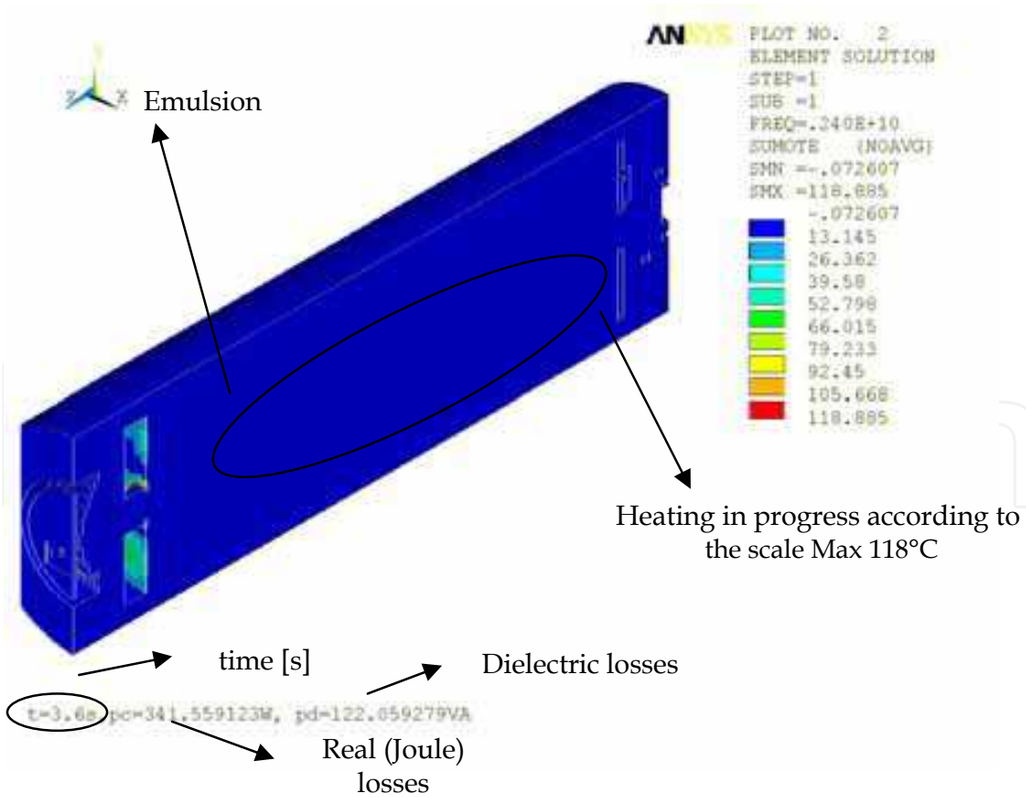

Fig. 31. The emulsion exsiccation process depending on time; emulsion heating generated by the dielectric and Joule losses; the distribution of temperature rise in the PCM model

5. Results of the thermal analysis

We may conclude that, in relation to the desiccated emulsion system, the numerical model enabled us to identify weak points of the design. These drawbacks consist in the fact that, under certain conditions, local spots might occur where uncontrolled temperature rise could result in explosion of the equipment. This status was experimentally verified.
Different variants of the reactor design were analyzed with the aim to evaluate the process and time of desiccation.
Even though modelling realized under the application of PCM produces certain theoretical complications, the actual model is reliable for the assumed boundary and initial conditions if the PCM macroscopic and microscopic properties are respected. This fact was verified experimentally and in laboratory conditions.

6. Acknowledgement

The research described in the paper was financially supported by the FRVS grant, research plan No MSM 0021630516, No MSM 0021630513.

7. References

Ansys User's Manual. Huston (USA): Svanson Analysys System, Inc., 1994-2011.

Baylin, F. (1979). *Low temperature thermal energy storage*. Golden (Colorado, USA): Solar Energy Research Institute Report No. SERI/RR-54-164.

BehuneK, I. (2004). *Operating features of accumulator for solar thermal energy storage*. In Student EEICT 2004, Bratislava: SUT in Bratislava, FEI.

Behunek, I. (2002). *Price analysis of electric heating*. In Czech, Master diploma work, DEEN, FEEC BUT, pages 72.

Behunek,I. (April 2004). *Solar system accumulation energy*. PhD thesis, BUT FEEC Brno, Czech Republic, vol. 10, pp. 41.

Behunek I, Fiala P. (Jun 2007). *Phase change materials for thermal management of IC packages*, Radioengineering Volume: 16 Issue: 2 Pages: 50-55.

Black out. (2003). http://www.cbsnews.com/stories/2003/08/15/national/main568422.shtml

Close, D.J., Dunkle, R.V. (1977). *Use of absorbent beds for energy storage in drying and heating systems*. Solar Energy 19.

Favier, A. (1999). *Almacenamiento de energia*. Dipatimento di Chimica-Fisica ed Elettrochimica, Universita degli Studi di Milano, Milano.

Fiala,P. (December 1998). Modeling of current transformers on a short- circuit. PhD thesis, VUT FEI Brno, vol. 13, ISBN 80-214-1346-8, pp. 41.

Fisher L.S. (1976). The *thermodynamics and some practical aspects of thermally layered heat storage in water*. Turnberry (Scotland): NATO Science Commitee Conference on Thermal Energy.

Garg, H.P., Mullick, S.C., Bhargava, A.K. (1985). *Solar Thermal Energy Storage*. Dordrecht (Holland): D. Reidel Publishing Company.

Gille, T.; Lisoni, J.; Goux, L.; De Meyer, K.; Wouters, D.J. (2007). *Modeling of the mechanical behavior during programming of a non-volatile phase-change memory cell using a coupled electrical-thermal-mechanical finite-element simulator*, Thermal, Mechanical and Multi-Physics Simulation Experiments in Microelectronics and Micro-Systems, 2007. EuroSime 2007. International Conference on Digital, Page(s): 1 - 6

Goldstein, M. (1961). *Some physical chemical aspects of heat storage*. Roma –Italy, UN Conference on New Source of Energy.

Jirku T, Fiala P, Kluge M. (May 2010). *Magnetic resonant harvesters and power management circuit for magnetic resonant harvesters*, Microsystem Technologies –Micro -and Nanosystems-Information Storage and Processing Systems, Volume: 16 Issue: 5 Special Issue: Sp. Iss. SI Pages: 677-690

John Greenman, Chris Melhuish, John Hart. (May 2005). *Energy accumulation and improved performance in microbial fuel cells,* Elsevier, Accepted 10 November 2004, Available online 31 May 2005.

Junrui Liang; Wei-Hsin Liao. (2010). *Impedance analysis for piezoelectric energy harvesting devices under displacement and force excitations,* Information and Automation (ICIA), 2010 IEEE International Conference on Digital Object, Page(s): 42 - 47

Juodkazis, Saulius; Misawa, Hiroaki; Maksimov, Igor. (November 2004). *Thermal accumulation effect in three-dimensional recording by picosecond pulses*, Applied Physics Letters, vol.85, no.22, pp.5239-5241.

Key World Energy Statistics from the IEA. (2002). Paris (France): The International, Energy Agency (IEA).

Leczek, J., (1981) *Solar energy-introduction to helioenergetics*. Prague: Redaction of elektrotechnical literature, In Czech.

Lane, G.A. (1983). *Solar Heat Storage*, Volume I: Background and Scientific Principles. Boca Raton (Florida, USA): CRC Press, Inc.

Lavan, Z., Thomson, J. (1977). *Experimental study of thermally stratified hot water storage tanks*. Solar Energy 19.

Lienhard, J.H. IV, Lienhard, J.H. V. (2004). *A heat transfer textbook*. Cambridge (Massachusetts, USA): Phlogiston Press.

Liu, Y.-T.; Lee, M.H.; Chen, H.T.; Huang, C.-F.; Peng, C.-Y.; Lee, L.-S.; Kao, M.-J. (2008). *Thermal accumulation improvement for fabrication manufacturing of monolithic 3D integrated circuits*, Solid-State and Integrated-Circuit Technology. ICSICT 2008. 9th International Conference on , vol., no., pp.1207-1210.

Mar, R.W. (1978). Material *problems in reversible chemical reaction storage systems for solar energy*. Report No. SAND 78-8693. Sandia Laboratories.

Mar, R.W. (1980). *Materials science issues encountered during the development of thermochemical concept*. In chapter 14 from the book, Solar materials science. London (UK): Academic Press, Inc.

Mar, R.W., BRamletta, T.T. (1980). *Thermochemical storage systems*. New York (USA): Marcel Dekker, Inc.

Ministery of industry and trade of Czech Republic, Stat energetic conception. Prague, 2004.

Ministery of industry and trade of Czech Republic, Energetic policy. Prague, 2000.

Mechlova, E., Kostal, K. (1999). *Physics dictionary for basic university physics lectures*. Prague: Prometheus.

Murat Kenisarin, Khamid Mahkamov. (May 2006). *Solar energy storage using phase change materials*, School of Engineering, University of Durham, Elsevier, Received 27 March 2006; accepted 8 May 2006

Piszachich, W.S. (1985). *Nonlinear Models of Flow, Diffusion and Turbulence*. Leipzig (Germany): Teubner Verlagsgessellschaft.

Shi, L.P.; Chong, T.C.; Wei, X.Q.; Zhao, R.; Wang, W.J.; Yang, H.X.; Lee, H.K.; Li, J.M.; Yeo, N.Y.; Lim, K.G.; Miao, X.S.; Song, W.D. (2006). *Investigation of Nano-Phase Change for*

Phase Change Random Access Memory, Non-Volatile Memory Technology Symposium, 2006. NVMTS 2006. 7th Annual, Digital Object, Page(s): 76 - 80

Solar energy, (2010), www.ausra.com

The Australian National University (2004), Department of Engineering, FEIT, http://solar.anu.edu.au/.

Vener, C. (1997). *Phase change thermal energy storage*. The Department of The Built Environment Brighton, University of Brighton, Brighton.

Verdonschet, J.K.M. (1981). *Thermal storage system based on the heat of adsorption in air-based solar heating system.* The Hague (Holland): C. Den Ouden.

Vijay Raghunathan; Kansal, A.; Hsu, J.; Friedman, J.; Mani Srivastava. (April 2005) *Design considerations for solar energy harvesting wireless embedded systems*, Information Processing in Sensor Networks, 2005. IPSN 2005. Fourth International Symposium on, vol., no., pp. 457- 462.

Vohlídal, Julák, Štulík. (1999). *Chemické a analytické tabulky*. In Czech, Prague: GRADA Publishing.

Volle, F.; Garimella, S.V.; Juds, M.A. (2010). *Thermal Management of a Soft Starter: Transient Thermal Impedance Model and Performance Enhancements Using Phase Change Materials*, Power Electronics, IEEE Transactions on, Volume: 25, Issue: 6, Page(s): 1395 - 1405.

Wilcox, D.C. (1994). *Turbulence modeling for CFD*. La Canada (California, USA): DCW Industries, Inc.

Zhen Ren; Wen-Yan Yin; Yan-Bing Shi; Qing Huo Liu. (Januar 2010). *Thermal Accumulation Effects on the Transient Temperature Responses in LDMOSFETs Under the Impact of a Periodic Electromagnetic Pulse*, Electron Devices, IEEE Transactions on, vol.57, no.1, pp.345-352.

Convection and Conduction Heat Transfer

Edited by Dr. Amimul Ahsan

ISBN 978-953-307-582-2
Hard cover, 394 pages
Publisher InTech
Published online 17, October, 2011
Published in print edition October, 2011

The convection and conduction heat transfer, thermal conductivity, and phase transformations are significant issues in a design of wide range of industrial processes and devices. This book includes 18 advanced and revised contributions, and it covers mainly (1) heat convection, (2) heat conduction, and (3) heat transfer analysis. The first section introduces mixed convection studies on inclined channels, double diffusive coupling, and on lid driven trapezoidal cavity, forced natural convection through a roof, convection on non-isothermal jet oscillations, unsteady pulsed flow, and hydromagnetic flow with thermal radiation. The second section covers heat conduction in capillary porous bodies and in structures made of functionally graded materials, integral transforms for heat conduction problems, non-linear radiative-conductive heat transfer, thermal conductivity of gas diffusion layers and multi-component natural systems, thermal behavior of the ink, primer and paint, heating in biothermal systems, and RBF finite difference approach in heat conduction. The third section includes heat transfer analysis of reinforced concrete beam, modeling of heat transfer and phase transformations, boundary conditions-surface heat flux and temperature, simulation of phase change materials, and finite element methods of factorial design. The advanced idea and information described here will be fruitful for the readers to find a sustainable solution in an industrialized society.

INTECH
open science | open minds

InTech Europe
University Campus STeP Ri
Slavka Krautzeka 83/A
51000 Rijeka, Croatia
Phone: +385 (51) 770 447
Fax: +385 (51) 686 166
www.intechopen.com

InTech China
Unit 405, Office Block, Hotel Equatorial Shanghai
No.65, Yan An Road (West), Shanghai, 200040, China
中国上海市延安西路65号上海国际贵都大饭店办公楼405单元
Phone: +86-21-62489820
Fax: +86-21-62489821

IntechOpen